Direction-of-Arrival Estimation and Cramer-Rao Bound for Multi-Carrier MIMO Radar

Michael Ulrich, Kilian Rambach and Bin Yang
Institute of Signal Processing and System Theory, University of Stuttgart
Pfaffenwaldring 47, 70550 Stuttgart, Germany
Tel.: +49 (0)711 685-67332, Fax: +49 (0)711 685-67311
Email: {michael.ulrich, kilian.rambach, bin.yang}@iss.uni-stuttgart.de

***Abstract*—Multi-carrier (MC) multiple-input multiple-output (MIMO) radar was recently applied to build sparse virtual arrays with a large aperture for a high-accuracy direction-of-arrival (DOA) estimation. The resulting grating lobes (DOA ambiguities) were resolved using multiple carriers. One problem of MC-MIMO is the coupling of the unknown parameters range and DOA. In this contribution, we study this range-DOA coupling for MC-MIMO systems. We consider both Cramer-Rao bound (CRB) of these parameters and their estimation. We show that a suitable choice of the coordinate system decouples range and DOA parameters in both CRB and estimation. This enables a sequential range and DOA estimation instead of a more complex joint estimation. Explanations of this phenomenon are given and simulation results confirm the theoretical findings.**

I. Introduction

It is well known, that the accuracy and ambiguity of the DOA estimation is determined by the positions of the antennas. On the one hand, a large aperture achieves a high estimation accuracy [1], [2], but on the other hand antennas must be placed close enough to avoid spatial aliasing (grating lobes) [3]–[5].

Common approaches to enhance the accuracy without spatial aliasing are sparse arrays and MIMO radar. In the former case, some antennas are placed close enough to avoid grating lobes and the remaining antennas are placed far away to achieve a large aperture at the price of increased sidelobes [4]. MIMO radar utilizes M transmit antennas (Tx) and N receive antennas (Rx) to create a virtual array with $M \times N$ elements [6]. This leads to a larger array aperture, while the hardware effort remains manageable [5].

The idea of using multiple carrier frequencies to improve DOA estimation has already been introduced in [7]. By using C different carrier frequencies, C scaled versions of the original array can be obtained without increasing the number of antennas. Angular ambiguities can then be resolved by using those scaled arrays. An algorithm using incoherent integration was presented in [8]. The drawback of the incoherent integration is that the sidelobe level is not smaller than $\frac{1}{C}$, where C is the number of carrier frequencies. Such high sidelobes are not desired in many applications.

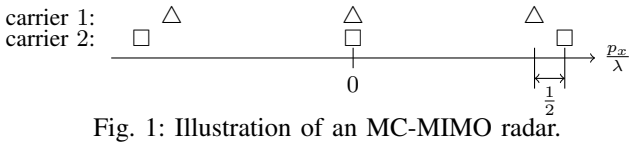

Fig. 1: Illustration of an MC-MIMO radar.

Novel design rules for such an array are presented in [9]. Fig. 1 illustrates the basic idea. It shows a linear array of three antennas placed far away to achieve a high aperture. The problem of spatial aliasing is solved by using multiple carrier frequencies. For a fixed antenna, a varying wavelength leads to a varying ratio of antenna position to wavelength. This means, the same antenna with different suitable carriers is able to satisfy the anti-aliasing condition.

A coherent processing of multi-carrier was applied to enhance the spatial resolution in [10], [11] and applied to Coarrays in [12], [13]. A coupling of the unknown parameters range and DOA is not considered in [10]–[13], thus those coherent algorithms are unsuitable for many applications.

The range-DOA coupling in multi-carrier MIMO is similar to the range-DOA coupling in frequency division multiplexing [14] and is described in [9], [15]. In a single-carrier radar, the range of a target appears as a fixed phase term in the baseband signal and does not interfere with the DOA estimation. In MC-MIMO, the same range leads to different phase changes for different carriers which are added to the DOA-induced phase changes in the baseband signal. [15] extends the multi-carrier signal model to MIMO and suggests a compensation technique for the range-DOA coupling, where the range is assumed to be known perfectly. As this is not practical in many applications, [9] presents a joint deterministic maximum likelihood (DML) estimator of range and DOA. A joint estimation requires a higher-dimensional search, which is computationally costly and therefore undesired.

In this paper, we study the range-DOA coupling of an MC-MIMO radar. We derive the joint CRB of both range and DOA and observe a decoupling in CRB by a suitable choice of the coordinate system. The same condition, if satisfied, also decouples the range and DOA estimation. This enables a sequential range and DOA estimation, namely a range estimation by pulse compression followed by a marginal DOA estimation using the MC-MIMO radar.

In this paper, we use the following notations: $\otimes$ is the Kronecker tensor product, while $\odot$ is the entrywise (Hadamard) product. $\underline{1}_K$ is a column vector consisting of K ones and $\mathbf{0}_{K\times K}$ is a square zero matrix of size $K \times K$. Furthermore, * denotes conjugate complex, ^{T} the transpose and ^{H} the Hermitian transpose. $\mathrm{diag}(\underline{a})$ is a diagonal matrix with the elements of $\underline{a}$ on the diagonal. $\mathbf{I}$ is the identity matrix and j the imaginary unit. The weighted sample correlation $\mathrm{Corr}^{\mathrm{WS}}$ between two matrices $\mathbf{A}$ and $\mathbf{B}$ and the weighted sample mean

978-0-9928-6265-7/16/$31.00 ©2016 IEEE

E^{WS} of $\mathbf{A}$ with the weight vector $\underline{w}$ are defined as in [2]:

$$\mathrm{Corr}^{\mathrm{WS}}(\mathbf{A},\mathbf{B},\underline{w}) := \frac{1}{\underline{1}^T\underline{w}}\mathbf{B}^H \,\mathrm{diag}(\underline{w})\mathbf{A}, \tag{1a}$$

$$\mathrm{E}^{\mathrm{WS}}(\mathbf{A},\underline{w}) := \frac{1}{\underline{1}^T\underline{w}}\underline{w}^T\mathbf{A}, \tag{1b}$$

The paper is organized as follows: We revise the MC-MIMO concept and its signal model for stationary targets in Sec. II. Our first contribution is the derivation of the CRB of the range and DOA parameters for an MC-MIMO radar in Sec. III. The second contribution is a suitable choice of the coordinate system which results in a decoupling of range and DOA estimation in Sec. IV. This leads to a simplified sequential range and DOA estimation with negligible performance degradation in comparison to the more complex joint range and DOA estimation. A comparison of the sequential DOA estimation, the joint deterministic maximum likelihood (DML) estimation and the CRB is given.

II. MC-MIMO Radar and Signal Model

In this paper, we make the following assumptions about the underlying MC-MIMO radar and targets:

- The MC-MIMO radar consists of M Tx and N Rx colocated antennas operating at C different carrier frequencies.
- The target is in the far field (colocated MIMO), i.e. the DOA is the same for all Tx and Rx antennas.
- All waveforms are orthogonal by using time or frequency or code division multiplex (TDM, FDM, CDM) [14]. They enable a $C \times M \times N$ virtual array. We do not discuss the multiplex details here.
- The radar uses a modulation like pulse Doppler or FMCW.
- An initial radar signal processing (pulse compression) is used to separate the targets in range domain, allowing a first coarse range estimation.
- In this paper, we consider a single stationary target in the far field in each range bin and focus on its DOA estimation. The more complicated case of moving targets and multiple targets in one range bin will be addressed in the future.

According to [6], [9], [16], the received continuous-time baseband signal for one target and the cmn-th channel consisting of the m-th Tx and n-th Rx antenna operating at the c-th carrier is

$$\tilde{x}_{cmn}(t) = \tilde{\alpha}_{cmn} s_{cmn}(t - (\tau_{\mathrm{Tx},m}(\underline{\theta}) + \tau_{\mathrm{Rx},n}(\underline{\theta}))\cdot \cdot \exp\left(-j2\pi f_c(\tau_{\mathrm{Tx},m}(\underline{\theta}) + \tau_{\mathrm{Rx},n}(\underline{\theta}))\right) + \tilde{n}_{cmn}(t), \tag{2}$$

$1 \le c \le C$, $1 \le m \le M$, $1 \le n \le N$. $s_{cmn}(t)$ is the sent signal at time t. $\tilde{\alpha}_{cmn}$ represents the complex amplitude of the received signal determined by the transmission power, propagation loss, radar cross-section (RCS) of the target and antenna gain. f_c is the c-th carrier frequency. The propagation delays from the m-th Tx antenna to the target and from the target to n-th Rx antenna are $\tau_{\mathrm{Tx},m}(\underline{\theta})$ and $\tau_{\mathrm{Rx},n}(\underline{\theta})$, where $\underline{\theta}$ contains the range and DOA parameters of the target. $\tilde{n}_{cmn}(t)$ is the noise.

After pulse compression and sampling, the received signal in one range bin is

$$x_{cmn}(l) = \alpha_{cmn}\exp\left(-j2\pi f_c(\tau_{\mathrm{Tx},m}(\underline{\theta}) + \tau_{\mathrm{Rx},n}(\underline{\theta}))\right) + + n_{cmn}(l), \qquad 1 \le l \le L \tag{3}$$

where L is the number of measurements (e.g. FMCW ramps) within one measurement cycle.

The delays $\tau_{\mathrm{Tx},m}$ and $\tau_{\mathrm{Tx},n}$ can be expressed as

$$\tau_{\mathrm{Tx},m}(\underline{\theta}) = \frac{r}{c} - \frac{1}{c}\underline{p}_{\mathrm{Tx},m}^T\underline{u}, \tag{4a}$$

$$\tau_{\mathrm{Rx},n}(\underline{\theta}) = \frac{r}{c} - \frac{1}{c}\underline{p}_{\mathrm{Rx},n}^T\underline{u}. \tag{4b}$$

r is the range of the target with respect to the origin of the coordinate system. We assume a planar antenna array located in the xy-plane of the coordinate system. $\underline{u} = [u_x, u_y]^T \in \mathbb{R}^2$ is the normalized direction vector pointing from the origin to the target and contains the electrical angles u_x and u_y. $\underline{p}_{\mathrm{Tx},m} \in \mathbb{R}^2$ and $\underline{p}_{\mathrm{Rx},n} \in \mathbb{R}^2$ denote the positions of the m-th Tx and n-th Rx antenna.

Stacking the signals of all channels x_{cmn} into one column vector $\underline{x}$ yields

$$\begin{aligned}\underline{x}(l) &= [x_{111}(l), ..., x_{11N}(l), ..., x_{1MN}(l), ..., x_{CMN}(l)]^T \\ &= \underline{\alpha} \odot \exp(j\mathbf{B}\underline{\theta}) + \underline{n}(l) \\ &:= \underline{a}(\theta) + \underline{n}(l)\end{aligned} \tag{5}$$

with

$$\mathbf{B} = \frac{2\pi}{c}\underline{f} \otimes \mathbf{Q}, \tag{6}$$

$$\mathbf{Q} = [\mathbf{P}, -2\,\underline{1}_{MN}], \tag{7}$$

$$\mathbf{P} = \mathbf{P}_{\mathrm{Tx}} \otimes \underline{1}_N + \underline{1}_M \otimes \mathbf{P}_{\mathrm{Rx}}, \tag{8}$$

$$\underline{\theta} = [u_x, u_y, r]^T. \tag{9}$$

$\underline{\alpha}$ represents the complex amplitude of the baseband signal. The notation $\exp(j\mathbf{B}\underline{\theta})$ is an elementwise application of $\exp(\cdot)$ to each element of $j\mathbf{B}\underline{\theta}$. $\underline{f} = [f_1, ..., f_C]^T$ is the vector of different carrier frequencies. The rows of $\mathbf{P}_{\mathrm{Tx}} \in \mathbb{R}^{M\times 2}$ and $\mathbf{P}_{\mathrm{Rx}} \in \mathbb{R}^{N\times 2}$ are $\underline{p}_{\mathrm{Tx},m}^T$ and $\underline{p}_{\mathrm{Tx},n}^T$. $\mathbf{P} \in \mathbb{R}^{MN\times 2}$ is the matrix containing the antenna positions of the $M \times N$ single-carrier virtual array, see [9] for details. In comparison, the multi-carrier virtual array by taking $\underline{f}$ into account has a size of $C \times M \times N$.

For the special case of a single Tx antenna ($M = 1$) and a linear Rx array, the coordinate system can be defined such that all CMN virtual antennas lie on the x-axis. The above signal model then simplifies to

$$\mathbf{P} = p_{x,\mathrm{Tx}}\underline{1}_N + \underline{p}_{x,\mathrm{Rx}}, \tag{10}$$

$$\underline{\theta} = [u_x, r]^T. \tag{11}$$

III. Cramer-Rao Bound

For the derivation of the Cramer-Rao Bound (CRB) of $\underline{\theta}$, we assume a sequence of i.i.d. circular complex zero-mean Gaussian noise samples $\underline{n}(l)$ with covariance $\sigma^2\mathbf{I}$ in Eq. 5. The CRB is given in [17]:

$$\mathrm{CRB}^{-1} = 2L\frac{1}{\sigma^2}\,\mathrm{Re}\{\mathbf{C}\}, \tag{12}$$

$$\mathbf{C} = \mathbf{D}^H \left(\mathbf{I} - \underline{a}(\underline{a}^H\underline{a})^{-1}\underline{a}^H\right)\mathbf{D} = \mathbf{D}^H\mathbf{D} - \mathbf{D}^H\frac{\underline{a}\ \underline{a}^H}{||\underline{a}||^2}\mathbf{D}. \tag{13}$$

For a compact formulation, we drop the the dependence of $\underline{a} = \underline{a}(\underline{\theta})$ of $\underline{\theta}$ in this section. $\mathbf{D}$ contains the derivatives of $\underline{a}$ with respect to $\underline{\theta}$

$$\mathbf{D} = \left[\frac{\partial \underline{a}}{\partial u_x}, \frac{\partial \underline{a}}{\partial u_y}, \frac{\partial \underline{a}}{\partial r}\right] \in \mathbb{C}^{CMN\times 3}. \tag{14}$$

After some calculations, we obtain

$$\mathbf{D} = j\mathbf{B} \odot [\underline{a}, \underline{a}, \underline{a}]. \tag{15}$$

The k-th column of $\mathbf{D}$ is thus $j\underline{b}_k \odot \underline{a}$ where $\underline{b}_k$ is the k-th column of $\mathbf{B}$ ($1 \le k \le 3$). Hence

$$\left[\mathbf{D}^H\mathbf{D}\right]_{ki} = (j\underline{b}_k \odot \underline{a})^H(j\underline{b}_i \odot \underline{a}) = \underline{b}_k^H \operatorname{diag}(\underline{\rho})\underline{b}_i \tag{16}$$

where $\underline{\rho} = \underline{\alpha}^* \odot \underline{\alpha} \in \mathbb{R}^{CMN}$ is the vector of signal powers of all CMN channels. This means,

$$\mathbf{D}^H\mathbf{D} = \mathbf{B}^H \operatorname{diag}(\underline{\rho})\mathbf{B} = \rho\,\mathrm{Corr}^{\mathrm{WS}}(\mathbf{B}, \mathbf{B}, \underline{\rho}) \in \mathbb{C}^{3\times 3} \tag{17}$$

with $\rho = \underline{1}^T\underline{\rho} = ||\underline{\alpha}||^2$ being the total signal power of all channels. Similar to Eq. 17, we calculate

$$\underline{a}^H\mathbf{D} = j\rho\,\mathrm{Corr}^{\mathrm{WS}}(\mathbf{B}, \underline{1}_{CMN}, \underline{\rho}) = j\rho\,\mathrm{E}^{\mathrm{WS}}(\mathbf{B}, \underline{\rho}). \tag{18}$$

$\mathbf{C}$ can then be calculated as

$$\mathbf{C} = \rho\left(\mathrm{Corr}^{\mathrm{WS}}(\mathbf{B}, \mathbf{B}, \underline{\rho}) - \mathrm{E}^{\mathrm{WS}}(\mathbf{B}, \underline{\rho})^H\,\mathrm{E}^{\mathrm{WS}}(\mathbf{B}, \underline{\rho})\right). \tag{19}$$

In the following, we assume that the signal power vector $\underline{\rho}$ is separable, i.e. $\underline{\rho} = \underline{\rho}_f \otimes \underline{\rho}_p$ with $\underline{\rho}_f \in \mathbb{R}^C$ and $\underline{\rho}_p \in \mathbb{R}^{MN}$. This condition is equivalent to $\rho_{cmn} = \rho_c\rho_{mn}$ and is usually satisfied. It means that each carrier can have a different transmission power ρ_c, but the powers ρ_{mn} for different Tx-Rx antenna combinations remain the same. $\mathbf{C}$ can then be expressed as

$$\mathbf{C} = \rho\left(\frac{2\pi}{c}\right)^2\Big[\mathrm{Corr}^{\mathrm{WS}}(\underline{f}, \underline{f}, \underline{\rho}_f)\,\mathrm{Corr}^{\mathrm{WS}}(\mathbf{Q}, \mathbf{Q}, \underline{\rho}_p) - \\ - \left(\mathrm{E}^{\mathrm{WS}}(\underline{f}, \underline{\rho}_f)\right)^2\mathrm{E}^{\mathrm{WS}}(\mathbf{Q}, \underline{\rho}_p)^H\,\mathrm{E}^{\mathrm{WS}}(\mathbf{Q}, \underline{\rho}_p)\Big]. \tag{20}$$

Let us now define

$$\underline{p}_0 = \frac{1}{2}\,\mathrm{E}^{\mathrm{WS}}(\mathbf{P}, \underline{\rho}_p)^T \in \mathbb{R}^2 \tag{21}$$

the position of the physical array centroid in the coordinate system. In the simple case of equal powers $\underline{\rho}_p \propto \underline{1}_{MN}$,

$$\underline{p}_0 = \frac{1}{2}\left(\frac{1}{M}\sum_{m=1}^{M}\underline{p}_{\mathrm{Tx},m} + \frac{1}{N}\sum_{n=1}^{N}\underline{p}_{\mathrm{Rx},n}\right)$$

is the arithmetic mean of the Tx array centroid and the Rx array centroid. Note that the centroid of the $M \times N$ single-carrier virtual array is $\mathrm{E}^{\mathrm{WS}}(\mathbf{P}, \underline{\rho}_p)^T = 2\underline{p}_0$, as $\underline{p}_0$ appears twice in the virtual array, see Eq. 8.

Then we introduce the centralized Tx and Rx antenna positions $\bar{\mathbf{P}}_{\mathrm{Tx}} = \mathbf{P}_{\mathrm{Tx}} - \underline{1}_M \otimes \underline{p}_0^T$ and $\bar{\mathbf{P}}_{\mathrm{Rx}} = \mathbf{P}_{\mathrm{Rx}} - \underline{1}_N \otimes \underline{p}_0^T$. This corresponds to a shift of the coordinate system origin of $\underline{p}_0$. According to Eq. 8,

$$\bar{\mathbf{P}} = \mathbf{P} - 2\underline{1}_{MN} \otimes \underline{p}_0^T. \tag{22}$$

Clearly, the new coordinate system origin at $\underline{p}_0$ is characterized by $\mathrm{E}^{\mathrm{WS}}(\bar{\mathbf{P}}, \underline{\rho}_p) = \underline{0}^T$. After some lengthly calculations (details omitted), we can show that

$$\mathrm{CRB} = \frac{1}{2L}\frac{\sigma^2}{\rho}\left(\frac{c}{2\pi}\right)^2\begin{bmatrix} \frac{1}{\gamma_2}\bar{\mathbf{E}}^{-1} & \frac{1}{\gamma_2}\bar{\mathbf{E}}^{-1}\underline{p}_0 \\ \frac{1}{\gamma_2}\underline{p}_0^T\bar{\mathbf{E}}^{-1} & \frac{1}{\gamma_2}\underline{p}_0^T\bar{\mathbf{E}}^{-1}\underline{p}_0 + \frac{1}{4\gamma_1}\end{bmatrix} \tag{23}$$

where $\bar{\mathbf{E}} = \mathrm{Corr}^{\mathrm{WS}}(\bar{\mathbf{P}}, \bar{\mathbf{P}}, \underline{\rho}_p)$ is the weighted sample correlation matrix of $\bar{\mathbf{P}}$, $\gamma_2 = \mathrm{E}^{\mathrm{WS}}(\underline{f}\odot\underline{f}, \underline{\rho}_f)$ is the weighted sample power of $\underline{f}$, and $\gamma_1 = \gamma_2 - (\mathrm{E}^{\mathrm{WS}}(\underline{f}, \underline{\rho}_f))^2$ is the weighted sample variance of $\underline{f}$.

The expression in Eq. 23 shows that the 3×3 CRB of $\underline{\theta}$ is block diagonal if $\underline{p}_0 = \underline{0}$. The CRB of the DOA parameters $\underline{u}$ and that of the range r are decoupled, if we choose the physical array centroid $\underline{p}_0$ to be the origin of the coordinate system. The choice of $\underline{p}_0$ also has an influence to the CRB of range, but it has no impact to the CRB of DOA as expected.

IV. DOA estimation for MC-MIMO Radar

A. Joint maximum likelihood estimation of range and DOA

The task of DOA estimation is the retrieval of $\underline{u}$ from the signal $\underline{x}(l)$. In the single-carrier case, the range causes a constant phase shift for all channels and can therefore be treated as an additional phase component of the amplitude $\underline{\alpha}$. This makes the single-carrier DOA-estimation independent of range.

This is not the case in MC-MIMO. The range induces a different phase shift for every carrier. Therefore, the range and DOA parameters should be jointly estimated in general. An extension of the DML estimator in [18] to joint DOA and range estimation is given in [9]. For L measurements, the joint DML estimator is

$$\hat{\underline{\theta}} = \arg\max_{\underline{\theta}}\phi(\underline{\theta}), \\ \phi(\underline{\theta}) = \left|\left|(\underline{a}(\underline{\theta}))^H\left(\sum_{l=1}^{L}\underline{x}(l)\right)\right|\right|^2. \tag{24}$$

However, it has a high computational complexity due to a 3-dimensional search. Even if the MC-MIMO uses a frequency modulation (e.g. pulse Doppler, FMCW) which allows an initial pulse compression to separate the targets in the range domain, the range estimation error may degrade the DOA estimation due to their coupling. At the end, a joint estimation as in Eq. 24 could be still necessary despite of an initial range estimation.

B. Locally decoupled DOA estimation

It would be nice if the range and DOA parameters are decoupled in the estimation. This implies that the residual estimation error in an initial coarse range estimation will not affect the DOA estimation. As a result, r and $\underline{u}$ can be

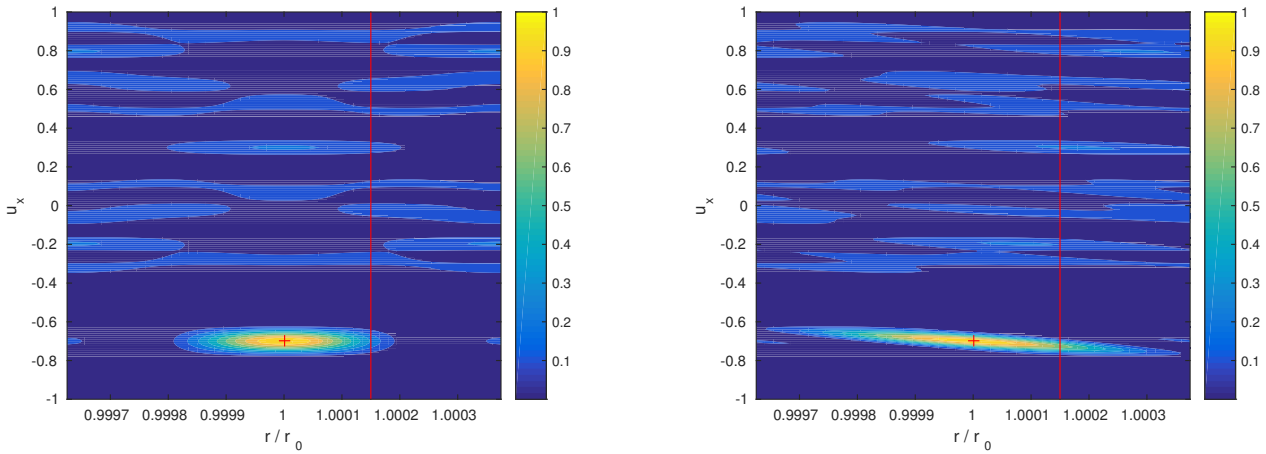

(a) The condition $\underline{p}_0 = \underline{0}$ is satisfied. This results in a local decoupling of the range and DOA.

(b) The condition $\underline{p}_0 = \underline{0}$ is violated. This results in a range-DOA coupling.

Fig. 2: Noise-free DML function $\phi(\underline{\theta})$ for an MC-MIMO radar for two different coordinate systems.

estimated sequentially, reducing the computational complexity to the single-carrier case. This means

$$\hat{\underline{u}} = \arg\max_{\underline{u}} \phi([\underline{u}^T, \hat{r}]^T), \tag{25}$$

where $\hat{r}$ is an initial estimate from pulse compression. In Sec. III, the condition $\underline{p}_0 = \underline{0}$ makes the CRB block diagonal. This implies a decoupling between $\underline{u}$ and r in the CRB. This motivates a similar study of range-DOA coupling in the estimation. For this purpose, the following simulation is conduced. A 3-carrier MIMO system with the carrier frequencies $\underline{f}_{\text{MC}} = [0.6f_0, 0.8f_0, f_0]^T$ is used where f_0 is any nominal carrier frequency. One simple transmitter ($M = 1$) and one receiving uniform linear array (ULA) with $N = 5$ antennas along the x-axis are used. The antenna spacing of the Rx array is $5 \cdot \frac{1}{2}\lambda_0 = 5\frac{c}{2f_0}$, which is much larger than the minimum spacing $\frac{1}{2}\lambda_0$ for a single-carrier radar [9]. Grating lobes due to the larger antenna spacing are resolved by the multi-carrier concept. A single stationary target is located at the true range $r_0 = 4000\lambda_0$ (far field) and true DOA $u_{x,0} = -0.7$. For simplicity, we assume equal amplitudes $\underline{\alpha} \propto \underline{1}_{CMN}$. The number of measurements is $L = 1$.

We plot the noise-free DML function $\phi(\underline{\theta})$ in Eq. 24 for this scenario for two different coordinate systems, see Fig. 2. The red $+$ indicates the true target and the vertical red line shows one possible coarse range estimate. In Fig. 2(a), the condition $\underline{p}_0 = \underline{0}$ is satisfied, i.e. the physical array centroid serves as the origin of the coordinate system. Clearly, the range and DOA estimations are locally decoupled. Even starting with a quite inaccurate range estimate (red line), an one-dimensional search along u_x will return an accurate DOA estimate. In Fig. 2(b), the origin of the coordinate system is chosen in a distance of $16\lambda_0$ to the physical array centroid and in the same distance $r_0 = 4000\lambda_0$ to the target as before. As a comparison, the array aperture is $10\lambda_0$. In this case, the range and DOA parameters are coupled. As a result, the same coarse range estimate (red line) as in Fig 2(a) results an a poor DOA estimate. In addition, we see in Fig 2(b) that the estimation uncertainty (variance) in the u_x-direction is comparable to that in Fig 2(a), while in the range direction it is significantly increased. These observations agree with the prediction from the CRB in Sec. III.

At a first look, the observation of an influence of the choice of the coordinate system on the range-DOA coupling is surprising. According to Eq. 5-9, the baseband noise-free signal of the virtual array is

$$\underline{\alpha} \odot \exp\left(j\frac{2\pi}{c}\underline{f} \otimes (\mathbf{P}\underline{u} - 2r\underline{1}_{MN})\right) \tag{26}$$

Clearly, both range r and DOA parameters $\underline{u}$ contribute each to a phase change of $-2\frac{2\pi}{c}\underline{f} \otimes r\underline{1}_{MN}$ and $\frac{2\pi}{c}\underline{f} \otimes \mathbf{P}\underline{u}$. In the simple case of equal powers $\underline{\rho}_p \propto \underline{1}_{MN}$, if the virtual array centroid $\mathrm{E}^{\text{WS}}(\mathbf{P}, \underline{1}_{MN})$ is zero, both phase change vectors above are orthogonal because of $\underline{1}_{MN}^T\mathbf{P} = \underline{0}^T$. This means, the phase changes due to r and $\underline{u}$ happen in known orthogonal subspaces, making a decoupled range and DOA estimation possible. If $\mathrm{E}^{\text{WS}}(\mathbf{P}, \underline{1}_{MN}) \neq \underline{0}^T$, the phase changes due to r and $\mathbf{P}\underline{u}$ overlap to a certain degree, resulting in an interference of range and DOA estimation. In the case of unequal powers, $\underline{\rho}_p \not\propto \underline{1}_{MN}$, the phase changes due to r and $\underline{u}$ are orthogonal if the weighted virtual array centroid $\mathrm{E}^{\text{WS}}(\mathbf{P}, \underline{\rho}_p)$ is zero in order to take the different powers of Tx-Rx antenna combinations into account. In line of this argumentation, we now better understand the CRB in Eq. 23. The larger the physical array centroid $\underline{p}_0$ (equivalently the virtual array centroid $2\underline{p}_0$), the stronger the loss of orthogonality of phase changes due to range and DOA, and the stronger the range-DOA coupling.

C. Performance evaluation

We continue with the computer experiment in part IV-B and compare the root mean-square-error (RMSE) of the joint DML estimator (Eq. 24) and the sequential DOA estimator (Eq. 25) with the CRB. The setup of the MC-MIMO radar and the target are as in Sec IV-B. In addition, we assume a

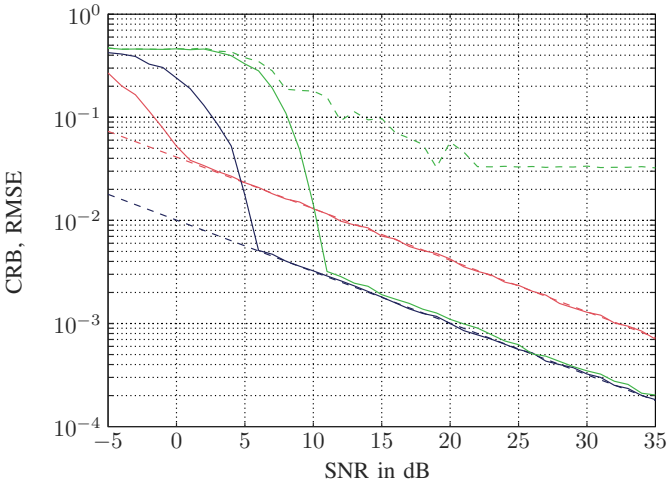

Fig. 3: CRB and RMSE of u_x. Dashed red and dashed blue: CRB of SC-MIMO and MC-MIMO. Solid red and solid blue: RMSE of SC-MIMO and MC-MIMO joint DML estimator. Solid green and dashed green: RMSE of sequential estimator, with $\underline{p}_0 = \underline{0}$ and $||\underline{p}_0|| = 16\lambda_0$.

linear FMCW modulation with a bandwidth of $B = 0.1f_0$ and 1024 samples per chirp. This enables a FFT-based pulse compression and an initial range estimate with an accuracy in the order of $10\lambda_0$, followed by an interpolation to obtain $\hat{r}$. For a comparison, a single-carrier MIMO radar with $\underline{f}_{\text{SC}} = [f_0, f_0, f_0]^T$ is simulated as well. In the Monte-Carlo simulations, 1000 independent trials have been done and the average RMSE as well as the CRB of u_x are plotted against the signal-to-noise ratio (SNR) after pulse compression in Fig. 3. Though in practical applications high SNRs are typical due to pulse compression, we also show the RMSE for DOA estimation at low SNR to demonstrate the threshold behaviour of MC-MIMO.

We make the following observations:

- The CRB of the MC-MIMO is significantly lower (about 12dB) than that of the single-carrier radar due to the larger antenna aperture of the multi-carrier concept.
- The DML-estimators for both single- and multi-carrier system asymptotically achieve their CRBs.
- The joint DML estimator of MC-MIMO has a higher SNR threshold compared to the single-carrier system due to the higher sidelobes of sparse virtual array of MC-MIMO, see [9].
- The sequential DOA estimator has a higher threshold than the joint DML estimator. This is due to the fact that the initial range estimate must hit the main peak of $\phi(\underline{\theta})$. The accuracy of the range estimation and, therefore, the FMCW bandwidth is limiting the sequential DOA estimation. This SNR threshold increases as the FMCW bandwidth decreases.
- The asymptotic variance of the sequential estimator is slightly higher than the CRB. This is due to the residual range estimation error, which leads to a SNR loss. In Fig. 2, the maximum of $\phi(\underline{\theta})$ along the red line has a lower amplitude than at the true range leading to a lower SNR.
- The RMSE of DOA in the sequential estimation with a non-central coordinate system is very poor. Due to the range-DOA coupling, the range estimation error degrades the DOA estimation dramatically.

V. Conclusion

We present in this paper the CRB of range and DOA for an MC-MIMO radar. Range and DOA coupling vanishes in the CRB for a certain choice of the coordinate system. We exploit the local decoupling of range and DOA to obtain a sequential DOA estimation, which is computationally less expensive than the joint DML estimator. The performance loss of this sequential estimation is much smaller than the significantly improved CRB of the MC-MIMO system compared to a single-carrier MIMO radar.

References

[1] P. Stoica and A. Nehorai, "MUSIC, Maximum Likelihood, and Cramer-Rao Bound," *IEEE Transactions on Audio and Electroacoustics*, vol. 37, pp. 720–741, May 1989.
[2] K. Rambach, M. Vogel, and B. Yang, "Optimal Time Division Multiplexing Schemes for DOA Estimation of a Target Using a Colocated MIMO Radar," in *IEEE International Symposium on Signal Processing and Information Technology*, 2014, pp. 108–113.
[3] M. Skolnik, *Radar Handbook*, M. Skolnik, Ed. McGraw Hill, 1990.
[4] H. L. V. Trees, *Optimum Array Processing*, H. L. V. Trees, Ed. Wiley, 2002.
[5] K. W. Forsythe and D. W. Bliss, *MIMO Radar Signal Processing*. John Wiley & Sons Inc, 2008, ch. 2, pp. 65–191.
[6] I. Bekkerman and J. Tabrikian, "Target Detection and Localization Using MIMO Radars and Sonars," *IEEE Transactions on Signal Processing*, vol. 54, pp. 3873–3883, Oct. 2006.
[7] M. Skolnik, "Resolution of angular ambiguities in radar array antennas with widely-spaced elements and grating lobes," *IRE Transactions on Antennas and Propagation*, vol. 10, no. 3, pp. 351–352, May 1962.
[8] M. J. Hinich, "Processing spatially aliased arrays," *Journal of the Acoustical Society of America*, vol. 64, no. 3, pp. 792–794, 1978.
[9] M. Ulrich and B. Yang, "Multicarrier MIMO Radar: A Concept of Sparse Array for Improved DOA Estimation," in *2016 IEEE Radar Conference*, Philadelphia, USA, May 2016.
[10] B. D. Steinberg and E. H. Attia, "Sidelobe Reduction of Random Arrays by Element Position and Frequency Diversity," *IEEE Transactions on Antennas and Propagation*, vol. AP-31, no. 6, pp. 922–930, November 1983.
[11] E. BouDaher, F. Ahmad, and M. G. Amin, "Sparse reconstruction for direction-of-arrival estimation using multi-frequency co-prime arrays," *EURASIP Journal on Advances in Signal Processing*, vol. 168, pp. 1–11, 2014.
[12] J. L. Moulton and S. A. Kassam, "Resolving more sources with multi-frequency coarrays in high-resolution direction-of-arrival estimation," in *43rd Annual Conference on Information Sciences and Systems (CISS)*, 2009, pp. 772–777.
[13] E. BouDaher, Y. Jia, F. Ahmad, and M. G. Amin, "Multi-Frequency Co-Prime Arrays for High-Resolution Direction-of-Arrival Estimation," *IEEE Transactions on Signal Processing*, vol. 63, no. 14, pp. 3797–3808, July 2015.
[14] H. Sun, F. Brigui, and M. Lesturgie, "Analysis and Comparison of MIMO Radar Waveforms," in *2014 International Radar Conference*, 2014.
[15] L. Zhuang and X. Liu, "Application of Frequency Diversity to Suppress Grating Lobes in Coherent MIMO Radar with Separated Subapertures," *EURASIP Journal on Advances in Signal Processing*, vol. 2009, pp. 1–10, 2009.
[16] J. Li and P. Stoica, "MIMO Radar with Colocated Antennas," *IEEE Signal Processing Magazine*, vol. 24, pp. 106–114, 2007.
[17] S. F. Yau and Y. Bresler, "A Compact Cramer-Rao Bound Expression for Parametric Estimation of Superimposed Signals," *IEEE Transactions on Signal Processing*, vol. 40, no. 5, pp. 1226–1230, May 1992.
[18] H. Krim and M. Viberg, "Two Decads of Array Signal Processing," *IEEE Signal Processing Magazine*, vol. 37, no. 5, pp. 720–740, May 1996.